Ab initio chemical kinetics for the ClOO + NO reaction: Effects of temperature and pressure on product branching formation

P. Raghunath and M. C. Lin

Citation: The Journal of Chemical Physics **137**, 014315 (2012); doi: 10.1063/1.4731883
View online: http://dx.doi.org/10.1063/1.4731883
View Table of Contents: http://scitation.aip.org/content/aip/journal/jcp/137/1?ver=pdfcov
Published by the AIP Publishing

Ab initio chemical kinetics for the ClOO + NO reaction: Effects of temperature and pressure on product branching formation

P. Raghunath and M. C. Lin[a)]
Center for Interdisciplinary Molecular Science, Department of Applied Chemistry, National Chiao Tung University, Hsinchu 300, Taiwan

(Received 5 March 2012; accepted 21 May 2012; published online 6 July 2012)

The kinetics and mechanism for the reaction of ClOO with NO have been investigated by *ab initio* molecular orbital theory calculations based on the CCSD(T)/6-311+G(3df)//PW91PW91/6-311+G(3df) method, employed to evaluate the energetics for the construction of potential energy surfaces and prediction of reaction rate constants. The results show that the reaction can produce two key low energy products ClNO + $^3O_2$ via the direct triplet abstraction path and ClO + NO_2 via the association and decomposition mechanism through long-lived singlet pc-ClOONO and $ClONO_2$ intermediates. The yield of ClNO + O_2 ($^1\Delta$) from any of the singlet intermediates was found to be negligible because of their high barriers and tight transition states. As both key reactions initially occur barrierlessly, their rate constants were evaluated with a canonical variational approach in our transition state theory and Rice–Ramspergen–Kassel–Marcus/master equation calculations. The rate constants for ClNO + $^3O_2$ and ClO + NO_2 production from ClOO + NO can be given by $2.66 \times 10^{-16}\ T^{1.91}\ \exp(341/T)$ (200–700 K) and $1.48 \times 10^{-24}\ T^{3.99}\ \exp(1711/T)$ (200–600 K), respectively, independent of pressure below atmospheric pressure. The predicted total rate constant and the yields of ClNO and NO_2 in the temperature range of 200–700 K at 10–760 Torr pressure are in close agreement with available experimental results. © *2012 American Institute of Physics*. [http://dx.doi.org/10.1063/1.4731883]

I. INTRODUCTION

Chlorine and chlorine oxide radicals play an important role in the destruction of atmospheric ozone in the polar stratosphere, through various photolytic or chemical processes.[1–3] The self-reaction of ClO radicals can produce ClOO, OClO, Cl, O_2, and Cl_2, in addition to the recombination products including the three isomers of Cl_2O_2. The reaction has been investigated extensively experimentally[3] and computationally.[4] Although the ClOO radical is short-lived as a result of its low Cl-O_2 bond energy of around 4.8 kcal/mol,[5–7] it has been considered to be a temporary sink for the Cl atoms at low temperature in the stratosphere. The kinetics for the formation of ClOO from Cl + O_2 reaction and decomposition of ClOO radicals have been investigated extensively both experimentally and theoretically.[5–14] Along with ClO_x radicals, NO_x (x = 1,2) are also very important in ozone destruction processes;[15] their interaction is of great relevance to the stratospheric chemistry.

For the interaction of the ClOO radical with NO, a subject of interest in the present work, Enami *et al.*[16] first measured the rate constant using the ultra-sensitive cavity ring-down spectrometry (CRDS) technique[17,18] by monitoring both ClOO and NO_2 in the temperature range of 205–243 K at pressures 50-150 Torr; they proposed the following reaction mechanism:

$$ClOO + NO \rightarrow ClNO + O_2, \quad (1)$$

$$\rightarrow ClONO_2, \quad (2)$$

$$\rightarrow ClO + NO_2. \quad (3)$$

The dominant products of the reaction were reported to be ClNO + O_2; the value for $k_{(ClOO+NO)}$ was measured to be $(4.5 \pm 0.9) \times 10^{-11}$ cm^3 molecules^{-1} s^{-1} at 213 K. Branching ratios of NO_2 and ClNO were concluded to be 0.18 ± 0.02 and ≈0.80, respectively at 213 K.[16]

The mechanism and kinetics of the related ClO + NO_2 reaction system, including its forward and reverse processes as well as the decomposition of its stable intermediate $ClONO_2$, have been studied in detail in 2005 at the CCSD(T)/6-311+G(3df)//B3LYP/6-311+G(3df) level of theory in conjunction with variational Rice–Ramspergen–Kassel–Marcus (RRKM) calculations.[19] In this work, we focused on the effects of temperature and pressure on chlorine nitrate formation and decomposition. The heats of formation of many of unstable intermediates such as ClOONO isomers have been predicted in this study. At the time, the importance of the ClOO + NO reaction in the stratosphere was not recognized as the kinetics and mechanism for the reaction were not available. In 2006, the excellent work of Enami *et al.*[16] on the kinetics of the ClOO + NO reaction employing the CRDS technique to measure the decay rate of ClOO and the production rate of NO_2 revealed very significantly that the ClOO + NO reaction occurred at a near gas-kinetic rate, but not forming the expected NO_2 product by the obvious radical-radical head-to-head association/

a)Author to whom correspondence should be addressed. Electronic mail: chemmcl@emory.edu.

decomposition mechanism. The authors suggested that as much as 80% of the "dark products" undetectable by their CRDS probing laser should be ClNO and O_2 most likely produced by the head-to-tail abstraction reaction.

In light of the interesting result of the ClOO + NO reaction by Enami *et al.*[16] on the production of the ClNO and NO_2 metathetical products, from the Cl-atom and the terminal O-atom abstractions by NO, respectively, as aforementioned, we have carried out a comprehensive *ab initio* quantum calculations to study the reaction system and clarify the mechanism involved. The computed potential energy surface and associated transition state parameters have been utilized to predict the rate constant as a function of temperature and pressure with variational transition state theory (TST) and/or multichannel (RRKM) theory for comparison with experimental values. The result is discussed in Secs. II–IV in detail.

II. COMPUTATIONAL METHODS

We have carried out the geometry optimization and energy prediction for all the molecules related to the ClOO + NO reaction using the GAUSSIAN 03 program.[20] The geometries of the reactants, intermediates, transition states, and products of the reaction were computed at the PW91PW91/6-311+G(3df) level with Perdew–Wang functionals[21,22] which have been shown to perform better than the commonly used B3LYP method for open-shell ClO_x molecules with less spin contaminations.[23] Theoretically, the optimized geometries, frequencies and heat of formation of ClOO radicals are calculated at various methods and compared with experimental data.[23,24] The differences in the bond length and bond angle of the radical between the predicted values with B3LYP/6-311+G(3df) and the experimental values reach as much as 0.422 Å and 6.5°, respectively. These deviations could be attributed to the large electron correlation effect in the ClOO radical. When PW91PW91/6-311+G(3df) method was used to optimize the geometry of ClOO in this work, the above differences were reduced to 0.16 Å and 6.6° with the Cl-O bond length closer to the experimental one. PW91PW91 provides more reasonable molecular geometries for ClOO comparing with experimental results.[23,24]

All geometries were analyzed by harmonic vibrational frequencies obtained at the same level to characterize stationary points and were used for the rate constant calculations. The transition state geometries were then used as an input for IRC calculations to verify the connectivity of the reactants and products.[25] For a more accurate evaluation of the energetic parameters, single-point energy calculations of the stationary points were carried out by the CCSD(T)/6-311+G(3df) method.[26]

For the entrance channel such as direct Cl-abstraction producing ClNO + $^3O_2$ and the formation of pc-ClOONO, the canonical variational transition-state theory (CVTST) (Refs. 27 and 28) approach was utilized to locate transition states for the key steps which occur without well-defined transition states. The rate constant and product branching ratios were computed with a microcanonical variational RRKM by the VARIFLEX program.[29] The component rates were evaluated at the E/J-resolved level and the pressure dependence was treated by one-dimensional master equation calculations using the Boltzmann probability of the complex for the J distribution.[30,31] For the barrierless association/decomposition process, either the individual points or the fitted Morse function, $V(\mathrm{R}) = D_e\{1 - exp[-\beta(R - R_e)]\}^2$, were used to represent the minimum potential energy path (MEP) which will be discussed later. Here, D_e is the bonding energy excluding zero-point vibrational energy for an association reaction, R is the reaction coordinate (i.e., the distance between the two bonding atoms), and R_e is the equilibrium value of R at the stable intermediate structure. For the tight transition states, the numbers of states were evaluated according to the rigid-rotor harmonic-oscillator approximation.

III. RESULTS AND DISCUSSION

A. Potential energy surfaces and reaction mechanism

The optimized geometries of the reactants, intermediates, transition states, and products as well as the available experimental values for them are shown in Fig. 1. The bond lengths and bond angles of these species optimized at the PW91PW91/6-311+G(3df) level are close to the experimental values.[24,32–33] The vibrational frequencies and

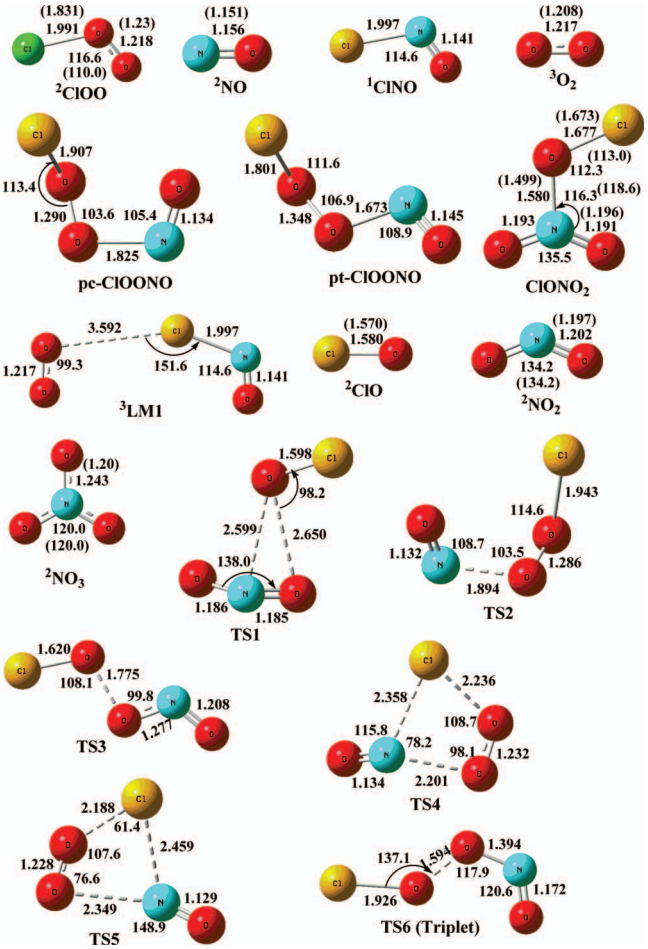

FIG. 1. The optimized geometries of the reactant, intermediates, transition states, and products computed at the PW91PW91/6-311+G(3df) level. The values in parenthesis are the experimental values (Refs. 24, 32–33). (Length in Å and angle in degree).

TABLE I. Calculated rotational constant and vibrational frequencies of the species involved in the ClOO + NO reaction computed at PW91PW91/6-311+G(3df) level of theory.

Species	B (GHZ)	Frequencies (cm^{-1})
^{2}ClOO	71.1, 5.3, 4.9	297, 516, 1418
^{2}NO	0.0, 50.7, 50.7	1897
^{1}ClNO	88.5, 5.6, 5.2	327, 598, 1842
$^3O_2$	0.0, 42.7, 42.7	1562
Pc-ClOONO	8.3, 2.6, 2.2	99, 207, 220, 299, 422, 550, 692, 1075, 1905
Pt-ClOONO	14.5, 1.8, 1.7	87, 169, 215, 298, 416, 533, 712, 960, 1850
$ClONO_2$	11.8, 2.7, 2.2	137, 225, 381, 519, 673, 744, 798, 1306, 1785
^{3}LM1	9.3, 1.0, 0.9	17, 23, 33, 33, 40, 328, 596, 1562, 1842
^{2}ClO	0.0, 18.4, 18.4	863
$^2NO_2$	236.9, 12.9,12.2	742, 1337, 1658
$^2NO_3$	13.6, 13.6, 6.8	487, 487, 774, 1086, 1229, 1229
TS1	10.8, 1.8, 1.6	*i*403, 48, 98, 123, 194, 657, 827, 1289, 1808
TS2	7.3, 2.5, 2.0	*i*159, 88, 199, 275, 327, 504, 568, 1091, 1914
TS3	37.3, 1.6, 1.5	*i*589, 58, 147, 267, 313, 738, 788, 866, 1536
TS4	4.4, 3.6, 2.1	*i*97, 153, 168, 275, 362, 404, 446, 1358, 1892
TS5	4.5, 3.3, 2.0	*i*126, 101, 222, 263, 336, 383, 531, 1373, 1928
TS6	20.4, 1.5, 1.4	*i*720, 63, 115, 197, 248, 387, 584, 804, 1671

rotational constant of all species are summarized in Table I. The potential energy diagram obtained at the CCSD(T)/6-311+G(3df)//PW91PW91/6-311+G(3df) level with zero point energy corrections is presented in Fig. 2 and the relative energies are calculated with respect to the reactants ClOO + NO.

The PES shown in Fig. 2 indicates that both Cl-abstraction and O-N association and dissociation reactions producing radical products occur without well-defined transition states. The dominating low energy reaction paths are discussed below.

Cl-atom abstraction: The Cl-abstraction reaction takes place without an intrinsic transition state through a triplet PES via van der Waals complex of the O_2 + ClNO products, OO · · ClNO (**LM1**), with Cs symmetry (see Figs. 1 and 2).

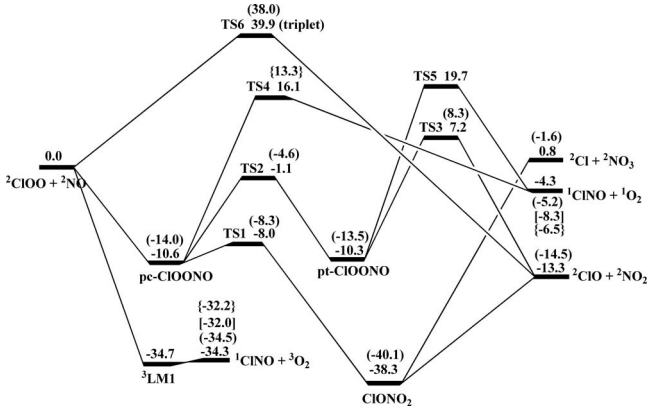

FIG. 2. Schematic energy diagram for the ClOO + NO reaction computed at the CCSD(T)/6-311+G(3df)//PW91PW91/6-311+G(3df) level with ZPE corrections. Relative energies are given in kcal/mol at 0 K. Data in the round bracket are predicted at CCSD(T)/6-311+G(3df)//B3LYP/6-311+G(3df) level from Ref. 19 and in square bracket at CASPT2/6-311+G(3df) //PW91PW91/6-311+G(3df) level of theory. Data in the curly bracket are predicted at G2M(RCC2)//PW91PW91/6-311+G(3df) method.

The complex is more stable than the ClOO + NO reactants by 34.7 kcal/mol at the CCSD(T)//PW91PW91 level. Formation of the complex LM1 occurs smoothly along the MEP by the concurrent shortening of the O_2Cl · · NO bond and the lengthening of the OO · · ClNO bond. LM1 has the O-Cl separation 3.592 Å and its geometrical parameters are almost equal to those in the ClNO + $^3O_2$ products with a small binding energy (0.4 kcal/mol). The ClNO and $^3O_2$ products with an overall exothermicity of 34.3 kcal/mol, which is close to the experimental heat of reaction, 32.5 ± 1 kcal/mol based on the experimental heats of formation ($\Delta_f H^\circ$) at 0 K for ClOO (23.8 ± 0.7 kcal/mol), NO (21.5 kcal/mol), ClNO (12.8 ± 0.1 kcal/mol), $^3O_2$ (0 kcal/mol) and $ClONO_2$ (7.9 ± 0.2 kcal/mol), ClO (24.2 ± 0.02 kcal/mol), NO_2 (8.6 ± 0.2), NO_3 (18.5 ± 5 kcal/mol), and Cl (28.6 kcal/mol).[32,34]

Association/dissociation reactions: In the initial steps of second mechanism, the terminal O atom of ClOO bonds with the reactive N atom in NO by a barrierless process forming pc-ClOONO which is an exothermic complexation process. The exothermicity is around 10.6 kcal/mol at the CCSD(T)//PW91PW91 level. Its related trans-type pt-ClOONO isomer is less stable by 0.3 kcal/mol. As shown in Fig. 1, the O-N bond lengths in pc-ClOONO and pt-ClOONO are 1.825 Å and 1.673 Å, respectively. As the reaction proceeds, pc-ClOONO intermediate can isomerize to the most stable intermediate $ClONO_2$ with a total exothermicity of 38.3 kcal/mol via TS1 with a small barrier of 2.6 kcal/mol. Barrier energy for same reaction was reported to be 6.7 kcal/mol by Zhu *et al.* at the CCSD(T)/6-311+G(3df)//B3LYP/6-311+G(3df) level.[19] The exothermicity for formation of $ClONO_2$ (38.3 kcal/mol) from ClOO + NO reaction is in good agreement with the experimental heat of reaction, −37.4 ± 0.7 kcal/mol.[32,34] In this potential energy surface, the cleavage of the O-N and O-Cl bond in the $ClONO_2$ isomer giving the products ClO + NO_2 and Cl + NO_3 is predicted to be endothermic by 25.0 and 39.1 kcal/mol, respectively. For the reaction ClOO + NO, the calculated heats of reaction for ClO + NO_2 and Cl + NO_3, −13.3 and −0.8 kcal/mol, are in reasonable agreement with the experimental values, −12.6 ± 0.7 and 1.83 ± 5.0 kcal/mol.[12] The isomerization between pc-ClOONO and pt-ClOONO occurs mainly through the rotation of the NO group, with a barrier of 9.5 kcal/mol. The corresponding transition state TS2 is presented in Fig. 2. After the isomerization of pt-ClOONO, it can further dissociate at the O-O bond to produce ClO + NO_2 with a barrier of 17.5 kcal/mol (or 7.2 kcal/mol above the reactants). The formation of ClNO + $^1O_2$ from pc-ClOONO and pt-ClOONO occurs via TS4 and TS5, in which the Cl atom migrates to the neighboring N atom with the high barriers of 16.1 and 19.7 kcal/mol, respectively, above the reactants (see Fig. 2). The direct abstraction formation of ClO + NO_2 from ClOO + NO requires a very high energy above the reactants via the triplet transition state TS6 (39.9 kcal/mol).

It should be mentioned that the formation of ClNO + O_2 ($^1\Delta$) on the singlet surface from pc-ClOONO via the four-member-ring TS4 is not competitive with the loose variational triplet TS path giving the triplet products, ClNO + O_2 ($^3\Sigma$), presented above because of the former's

tight structure with a high barrier (16.1 kcal/mol at the CCSD(T)/6-311+G(3df)//PW91PW91/6-311+G(3df) level and 13.3 kcal/mol by the G2M method[37]) above the reactants as shown in Fig. 2. The predicted heat of reaction, −4.3 kcal/mol, is as much as 30.0 kcal/mol above the triplet products. The computed singlet-triplet splitting for the O_2 is thus 7.5 kcal/mol higher than the experimental value. The deficiency of the single reference methods in predicting the singlet-splitting gap of O_2 is well-known.[35,36] Based on the geometries predicted at the PW91PW91/6-311+G(3df) level, however, the full valence CASPT2 method reduces the size of the splitting to 23.7 kcal/mol, which is much closer to the experimental value. We also calculated the singlet-triplet splitting energy difference to be 25.7 kcal/mol with the G2M(RCC2) method.

B. Rate constant calculation

The rate constants of the following low energy product channels are calculated by variational TST and RRKM rate theory using the energetics presented in Fig. 2 and the vibrational frequencies and rotational constants displayed in Table I.

$$\begin{aligned} &\mathrm{C1OO} + \mathrm{NO} \xrightarrow{\mathrm{VTS1}} \mathrm{C1NO} + {}^3\mathrm{O}_2 \quad (k_1)\\ &\mathrm{C1OO} + \mathrm{NO} \xrightarrow{\mathrm{VTS2}} \text{pc-C1OONO}^* \xrightarrow{\mathrm{TSI}} \mathrm{C1ONO}_2^* \longrightarrow \mathrm{ClONO}_2(+\mathrm{M}) \quad (k_2)\\ &\qquad\qquad\qquad\qquad\qquad\qquad\qquad\qquad \xrightarrow{\mathrm{VTS3}} \mathrm{C1O} + \mathrm{NO}_2 \quad (k_3), \end{aligned}$$

where * denotes the chemically activated species.

Variational approach: As stated above, for both the direct Cl-abstraction and the formation of pc-ClOONO, their initial steps occurring without well-defined transition states, we predicted their rate constants by using the CVTST approach[26,27] to locate their transition states based on the maximum Gibbs free energy criterion at each temperature. To evaluate the variational potential energy curves, the reaction pathways have been mapped out along the MEP with the tight convergence criterion and the projected frequency calculations were performed at the PW91PW91/6-311+G(3df). For instance, the MEP curve of the Cl-abstraction reaction forming LM1, OO · · ClNO, was obtained by varying the Cl-N bond distance from its equilibrium value (1.997 Å) at an interval of 0.1 Å, up to the separation at which the ClOO and NO fragments are completely separated at 4.5 Å. In order to obtain more reliable energies along the reaction path, we calculated the single-point energies, corrected by the second-order multireference perturbation theory (CASPT2)[31] based on the CASSCF optimized geometries with eight active electons and eight active orbitals with the 6-311+G(3df) basis set. These calculations are performed with the MOLPRO code.[38] In the same manner, we also located the loose transition states for the variational formation of the O-N bond in pc-ClOONO from ClOO + NO and the breaking of ClO · · NO_2 bond in $ClONO_2$. The resulting energies can be approximated with the Morse potential energy functions in units of kcal/mol:

$$\mathrm{VTS1}(R_{Cl\text{-}N}) = 34.7\{1 - \exp[-2.12(R - 1.99)]\}^2, \quad (4)$$

$$\mathrm{VTS2}(R_{O\text{-}N}) = 10.6\{1 - \exp[-2.32(R - 1.83)]\}^2, \quad (5)$$

$$\mathrm{VTS3}(R_{N\text{-}O}) = 27.8\{1 - \exp[-2.57(R - 1.58)]\}^2. \quad (6)$$

Using the Morse potential energies, computed moments of inertia and the vibrational frequencies of LM1 and pc-ClOONO parameters (see Tables S1 and S2 of the supplementary material[39]), we searched for maximum ΔG(T,s) or the transition state which is approximately located at each temperature. The approximate locations of the dividing surfaces by the CVTST method estimated Cl-N bond as 4.298 Å and 4.198 Å at 200–400 K and 500–700 K, respectively, for the formation of ClNO + O_2 via LM1. And similarly, for the formation of pc-ClOONO, the estimated O-N bond separation was 2.85 Å at 200–700 K. The Morse potential of VTS3 was determined to be $\beta = 2.57$ Å for the dissociation of $ClONO_2$. These values will be used in the following rate constant calculation to confirm the reliability of treating these barrierless processes.

The rate constant for the forward reaction of the low energy channels, ClOO + NO, have been computed in the temperature range of 200–700 K and the pressure range of 10–760 Torr with the Variflex code, whereas the higher energy channels are neglected. The VTST calculations were carried out with the unified statistical formulation of Miller[40] including multiple reflection corrections[41] above the shallow wells of the prereaction and postreaction complexes. The Lennard-Jones parameters employed for the ClOO + NO reaction are as follows: for LM1, $\varepsilon/k = 230$ K, and $\sigma = 4.2$ Å which are approximated to be the same as HOOClO system;[42] $ClONO_2$ isomers are taken to be $\varepsilon/k = 364.7$ K and $\sigma = 4.47$ Å (Ref. 43) and for buffer gas N_2, $\varepsilon/k = 82$ K and $\sigma = 3.74$ Å.[44] For the electronic partition functions ClO ($^2\Pi_{3/2}$ and $^2\Pi_{1/2}$) and NO ($^2\Pi$) the energy gap of 318 cm^{-1} and 121.1 cm^{-1}, respectively, between their two spin-orbit states have been taken into consideration.[32] The energy-transfer rate coefficients were computed on the basis of the exponential down model with the $\langle\Delta E\rangle_{down}$ value of 400 cm^{-1}. To achieve convergence in the integration over the energy range, an energy grain size of 100 cm^{-1} was used. This grain size provides

TABLE II. Three-parameter Arrhenius expressions[a] of predicted individual product rate constants (cm^3 $molecule^{-1}$ s^{-1}).

P (Torr)	T/K	ClNO + $^3O_2$ (k_1)
10–760	200–700	2.66×10^{-16} $T^{1.91}$ exp(341/T)
P (Torr)	**T/K**	**$ClONO_2$ (k_2)**
10	200–700	1.20×10^{-9} $T^{-4.37}$ exp(570/T)
50	200–700	5.49×10^{-9} $T^{-4.36}$ exp(574/T)
150	200–700	1.78×10^{-8} $T^{-4.37}$ exp(571/T)
300	200–700	3.36×10^{-8} $T^{-4.36}$ exp(574/T)
400	200–700	4.65×10^{-8} $T^{-4.37}$ exp(572/T)
760	200–700	9.16×10^{-8} $T^{-4.37}$ exp(570/T)
high-P	200–600	1.32×10^{-24} $T^{4.0}$ exp(1715/T)
P (Torr)	**T/K**	**ClO + NO_2 (k_3)**
10–760	200–600	1.48×10^{-24} $T^{3.99}$ exp(1711/T)
P (Torr)	**T/K**	**$k_{tot} = k_1 + k_2 + k_3$**
10–760	200–400	1.05×10^{-19} $T^{3.06}$ exp(746/T)
	400–700	2.61×10^{-15} $T^{1.60}$ exp(−201/T)

[a] $k(T) = AT^n \exp(-E_a/RT)$ predicted for various temperature range in unit of cm^3 $molecule^{-1}s^{-1}$.

numerically converged results for all temperature studies with the energy range spanning from 13 396 cm^{-1} below to 79 000 cm^{-1} above the threshold. The total angular momentum J covered the range from 1 to 250 in steps of 10 for the E- and J-resolved calculations.

ClOO + NO → ClNO + $^3O_2$: The rate constant for the ClOO + NO → ClNO + $^3O_2$ reaction by abstraction via LM1 was calculated in the temperature range of 200 to 700 K for comparison with the available experimental data measured by Enami *et al.*[16] using the cavity ring-down spectroscopy method in 50–150 Torr pressure of O_2/N_2 diluent at 205–243 K. As alluded to above, the transition states of the barrierless entrance treated by the CVTST approach were located at the Cl-N separation of 4.297 Å at 200–400 K and 4.197 Å at 500–700 K. In our calculations, the lowest vibrational modes 33.9 cm^{-1} and 33.99 cm^{-1} in both temperature regimes corresponding to the NO torsional motions, were treated as a one-dimensional free rotor. The predicted rate constants for the Cl-abstraction reaction for ClOO + NO → ClNO + $^3O_2$ (k_1) is a pressure-independent process as shown in Table II and Fig. 3 are given by the following three parameter expression covering the temperature range of 200–700 K at the 10–760 Torr pressure:

$$k_1 = 2.66 \times 10^{-16}\ T^{1.91}\ \exp(341/T) cm^3\ mol^{-1}\ s^{-1}$$

The experimentally measured rate constants for this reaction are 3.69×10^{-11} and 3.82×10^{-11} cm^3 $molecule^{-1}$ sec^{-1} at 213 K and 223 K, respectively;[16] they are in good agreement with our predicted values 3.78×10^{-11} and 3.83×10^{-11} cm^3 $molecule^{-1}$ sec^{-1}, respectively, at the two temperatures.

ClOO + NO → $ClONO_2$ and ClOO + NO → ClO + NO_2: The rate constants of these reactions have been treated with multiple reflections above the entrance well using the molecular parameters and the energies presented in Table I and Fig. 1. For the barrierless entrance pc-ClOONO association reaction, the CVTST approach with a free rotor for ClO gives rise to a transition state at the O-N separation of 2.85 Å at 200–700 K. For the rate constant calculation, the internal rotation of the NO group in pc-ClOONO is hindered by a 9.5 kcal/mol barrier. The barrier energy is calculated for isomerization between pc-ClOONO and pt-ClOONO occurring mainly through the rotation of the NO group. This vibrational mode (219 cm^{-1}) is thus treated as a hindered rotor. Also, the internal rotation of the ClO group with the vibrational frequency of 137 cm^{-1} at the $ClONO_2$ is hindered by a 7.3 kcal/mol barrier and thus also treated as a hindered rotor. Furthermore, the low frequencies at 99 cm^{-1} for pc-ClOONO, 48 cm^{-1} at TS1, 71 cm^{-1} for the entrance transition state estimated with the CVTS geometry were treated as free internal rotors. For the exit channel of $ClONO_2$ → ClO + NO_2 reaction, we used the Morse potential with $\beta = 2.57$. The results of our calculations are plotted in Figures 4 and 5 for the temperature range of 200–700 K and the pressure range of 10–760 Torr for comparison with all existing experimental data. The calculations show that below 760 Torr, formation of ClO + NO_2 from ClOO + NO is a pressure independent process. The calculated rate constant expressions for all the reaction product channels obtained by three-parameter

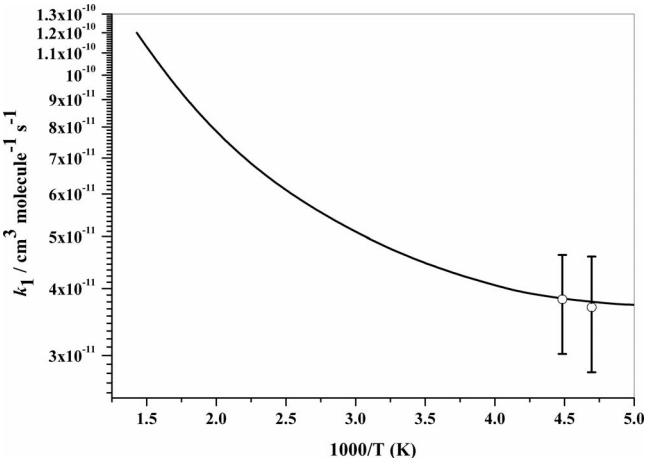

FIG. 3. Plot of predicted rate constant for ClOO + NO → ClNO + $^3O_2$ (k_1) channel with respect to temperature. Experimental data (O) at 213 and 223 K and 50–150 Torr pressure is taken from Ref. 16.

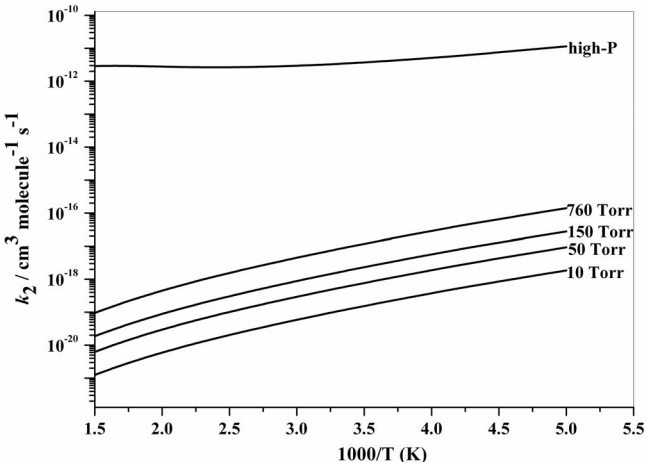

FIG. 4. Predicted rate constant for ClOO + NO → $ClONO_2$ (k_2) channel with respect to temperature and pressure.

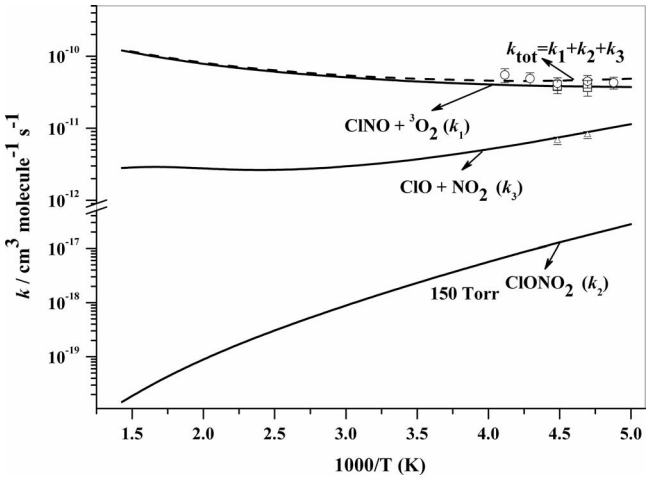

FIG. 6. Plot of predicted rate constant for individual product rate constant with respect to temperature and pressure at 150 Torr. Experimental data at 213–243 K and 50–150 Torr pressure is taken from Ref. 16.

fitting at 10–760 pressure range and 200–700 K temperature range are given in Table II. Recent results for ClOO + NO → ClO + NO_2 reaction measured by the CRDS technique in 50–150 Torr pressure at 213–243 K[16] are in good agreement with our predicted results. At 213 K, the experimental rate 8.1 × 10^{-12} cm^3 molecule^{-1} sec^{-1} compares closely with our predicted rate 8.8 × 10^{-12} cm^3 molecule^{-1} sec^{-1}. The $ClONO_2$ molecule was not detected experimentally; its yields under experimental conditions are predicted to be negligible. Figure 6 summarizes the total and individual product rate constants of the ClOO + NO reaction at the 10–760 Torr N_2 pressure to compare with experimental data.

Product branching ratios: The branching ratios for all product channels are shown in Fig. 7 as the functions of temperature and compared with experimental values measured for 50 Torr N_2 pressure. The results show that at temperature 213 and 223 K, the branching ratio of ClO + NO_2 yields are 0.19 and 0.16 which are in excellent agreement with experimental result 0.18 ± 0.02 and 0.15 ± 0.02, respectively. It is evident from Figure 7, channel 2 producing $ClONO_2$ (k_2) is noncompetitive and its branching ratio is zero throughout the entire temperature range. In Figure 7, the predicted branching ratio for ClNO formation is 77%–98% in the temperature range 200–700 K; this implies that the contribution from the direct Cl-abstraction process is predominant.

IV. CONCLUSIONS

The mechanism, rate constants, and product branching ratios for the ClOO + NO reaction have been investigated at the CCSD(T)/6-311+G(3df)//PW91PW91/6-311+G(3df) level of theory in conjunction with CVTST and RRKM calculations. The results show that the most favorable low energy products for the title reaction are ClNO + $^3O_2$, produced readily by NO abstracting the Cl atom from ClOO via the triplet ground state surface. This pressure-independent process occurs without an intrinsic barrier with the predicted rate constant $k_1 = 2.66 \times 10^{-16}\ T^{1.91} \exp(341/T)$ cm^3 molecule^{-1} sec^{-1} for 200–700 K. Another low energy product pair ClO + NO_2 occurs by a stepwise mechanism via the association of

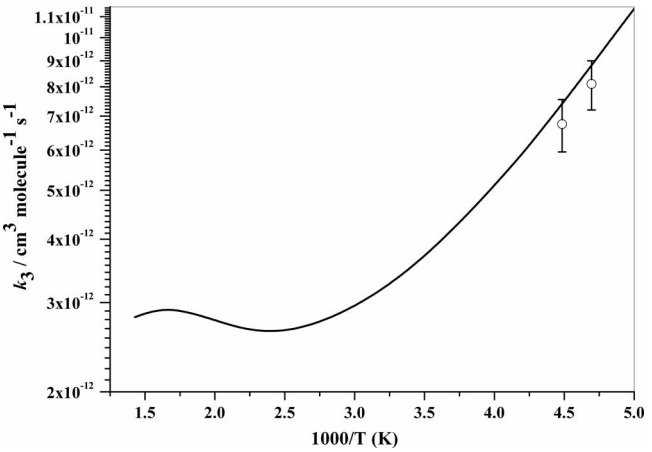

FIG. 5. Predicted rate constant for ClOO + NO → ClO + NO_2 (k_3) channel with respect to temperature at pressures (10–760 Torr). Experimental data (O) at 213 and 223 K and 50–150 Torr pressure is taken from Ref. 16.

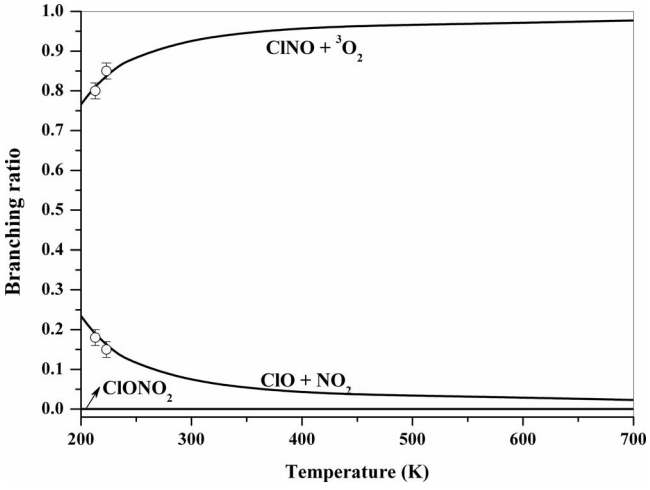

FIG. 7. Branching ratios of the products ClNO + $^3O_2$ (k_1), $ClONO_2$ (k_2) and ClO + NO_2 (k_3) as functions of temperature relative to the total rate constant k_{total} at pressure 50–150 torr N_2 bath gas with experimental values (Ref. 16).

the terminal O atom of ClOO with the reactive N atom in NO forming pc-ClOONO barrierlessly and subsequently followed by ClO migration to form the internally excited $ClONO_2$ intermediate with a 2.6 kcal/mol barrier. The excited $ClONO_2$ thus formed rapidly dissociates into the ClO + NO_2 products with no pressure effects below atmospheric pressure because of the relatively low ClO−NO_2 dissociation energy (25 kcal/mol) and the 13.3 kcal/mol overall exothermicity. The pressure independent rate constant for this reaction can be represented by $k_3 = 1.48 \times 10^{-24}\ T^{3.99}\ \exp(1711/T)\ cm^3\ molecule^{-1}\ sec^{-1}$ (200–600 K) for N_2 buffer gas. The branching ratios of the major product channels ClNO + $^3O_2$ (k_1) and ClO + NO_2 (k_3) account for 0.77–0.98 and 0.23–0.02 in the temperature range 200–700 K, respectively, agreeing very satisfactorily with experimental values. The channel producing $ClONO_2$ is negligible below atmospheric pressure over the entire range of temperature studied.

ACKNOWLEDGMENTS

The authors deeply appreciate the support of this work by the MOE ATU program. M.C.L. also wants to acknowledge the support from the Taiwan Semiconductor Manufacturing Company for the TSMC Distinguished Professorship and for the National Science Council of Taiwan for the Distinguished Visiting Professorship at National Chiao Tung University in Hsinchu, Taiwan. We are grateful to the National Center for High-performance computing for computer time and facilities. R. P. would also like to thank Dr. Z. F. Xu for useful discussions.

[1] J. G. Anderson, J. J. Margitan, and D. H. Stedman, Science **198**, 501 (1977).
[2] B. J. Finlayson-Pitts and J. N. Pitts, Jr., *Atmospheric Chemistry* Part 9, (Wiley Interscience, New York, 1986).
[3] L. T. Molina and M. J. Molina, J. Phys. Chem. **91**, 433 (1987); S. P. Sander, R. R. Friedl, and Y. L. Yung, Science **245**, 1095 (1989); M. B. McElroy, R. J. Salawitch, S. C. Wofsy, and J. A. Logan, Nature (London) **321**, 759 (1986).
[4] R. S. Zhu and M. C. Lin, J. Chem. Phys. **118**, 4094 (2003).
[5] J. M. Nicovich, K. D. Kreutter, C. J. Shackelford, and P. H. Wine, Chem.Phys. Lett. **179**, 367 (1991).
[6] S. Baer, H. Hippler, R. Rahn, M. Siefke, N. Seitzinger, and J. Troe, J. Chem. Phys. **95**, 6463 (1991).
[7] R. L. Mauldin III, J. B. Burkholder, and A. R. Ravishankara, J. Phys. Chem. **96**, 2582 (1992).
[8] M. P. Gane, N. A. Williams, and J. R. Sodeau, J. Chem. Faraday. Trans. **93**, 2747 (1997).
[9] C. L. Thomsen, M. P. Philpott, and S. C. Hayes, J. Chem. Phys. **112**, 505 (2000).
[10] B. J. Finlayson-Pitts, and J. N. Pitts, Jr., *Chemistry of the Upper and Lower Atmosphere: Theory, Experiments and Applications* (Academic, San Diego, CA, 2000).
[11] Q. Li, S. Lu, W. Xu, Y. Xie, and H. S. Schaefer, J. Phys. Chem. A **106**, 12324 (2002).
[12] R. S. Zhu and M. C. Lin, J. Chem. Phys. **119**, 2075 (2003); Comput. Theort. Chem. **965**, 328 (2011).
[13] K. Suma, Y. Sumiyoshi, Y. Endo, S. Enami, S. Hashimoto, M. Kawasaki, S. Nishida, and Y. Matsumi, J. Phys. Chem. A. **108**, 8096 (2004).
[14] K. Suma, Y. Sumiyoshi, and Y. Endo, J. Chem. Phys. **121**, 8351 (2004).
[15] P. J. Crutzen, Q. J. R. Meterol. Soc. **96**, 320 (1970); H. S. Johnston, Science **173**, 517 (1971); J. C. Farman, B. G. Gardiner and J. D. Shanklin, Nature (London) **315**, 207 (1985); R. S. Stolarski and R. J. Cicerone, Can. J. Chem. **52**, 1610 (1974); H. Sayin and M. L. McKee, J. Phys. Chem. A. **109**, 4736 (2005).
[16] S. Enami, Y. Hoshino, Y. Ito, S. Hashimoto, M. Kawasaki, and T. J. Wallington, J. Phys. Chem. A. **110**, 3546 (2006).
[17] M. D. Wheeler, S. M. Newton, A. J. Orr-Ewing, and M. N. R. Ashfold, J. Chem. Soc. Faraday Trans. **94**, 337 (1998); G. Berden, R. Peeters, and G. Meijer, Int. Rev. Phys. Chem. **19**, 565 (2000).
[18] T. Yu and M. C. Lin, Int. J. Chem. Kinet. **25**, 875 (1993); J. Phys. Chem. **99**, 8599 (1995).
[19] R. S. Zhu and M. C. Lin, Chem. Phys. Chem. **6**, 1514 (2005).
[20] M. J. Frisch, G. W. Trucks, and H. B. Schlegel *et al.*, GAUSSIAN 03, Revision C.02, Gaussian, Inc., Pittsburgh, PA, 2004.
[21] K. Burke, J. P. Perdew, and Y. Wang, in *Electronic Density Functional Theory: Recent Progress and New Direction* (Plenum, New York, 1998).
[22] J. P. Perdew, K. Burke, and Y. Wang, Phys. Rev. B **54**, 16533 (1996).
[23] R. S. Zhu and M. C. Lin, J. Chem. Phys. **134**, 054307 (2011); J. Phys. Chem. A **107**, 3836 (2003); **106**, 8386 (2002); M. Filatov and D. Cremer, Phys. Chem. Chem. Phys. **5**, 2320 (2003).
[24] A. Arkell and I. Schwager, J. Am. Chem. Soc. **89**, 5999 (1967).
[25] C. Gonzalez and H. B. Schlegel, J. Phys. Chem. **90**, 2154 (1989).
[26] J. A. Pople, M. Head-Gordon, and K. Raghavachari, J. Chem. Phys. **87**, 5968 (1987).
[27] A. Fernández-Ramos, J. A. Miller, S. J. Klippenstein, and D. G. Truhlar, Chem. Rev. **106**, 4518 (2006).
[28] C.-C. Hsu, A. M. Mebel, and M. C. Lin, J. Chem. Phys. **105**, 2346 (1996).
[29] S. J. Klippenstein, A. F. Wagner, R. C. Dunbar, D. M. Wardlaw, and S. H. Robertson, variflex: Version 1.00, 1999.
[30] R. G. Gilbert and S. C. Smith, *Theory of Unimolecular and Recombination Reactions* (Blackwell Scientific, Carlton, Australia, 1990).
[31] K. A. Holbrook, M. J. Pilling, and S. H. Robertson, *Unimolecular Reactions* (Wiley, New York, 1996).
[32] M. W. Chase, Jr., *NIST-JANAF Thermochemical Tables*, 4th ed., J. Phys. Chem. Ref. Data, No. 9 (1998).
[33] B. Casper, P. Lambotte, R. Minkvitz, and H. Oberhammer, J. Phys. Chem. **97**, 992 (1993).
[34] R. Alqasmi, H. D. Knauth, and D. Rohlack, Ber. Bunsenges. Phys. Chem. **82**, 217 (1978).
[35] C. Schweitzer and R. Schmidt, Chem. Rev **103**, 1685 (2003).
[36] R. S. Zhu, C. C. Hsu, and M. C. Lin, J. Chem. Phys **115**, 195 (2001); Y. Ge, K. Olsen, R. I. Kaiser, and J. D. Head, AIP Conf. Proc **855**, 253 (2005).
[37] A. Mebel, K. Morokuma, and M. C. Lin, J. Chem. Phys **103**, 7414 (1995).
[38] H.-J. Werner, P. J. Knowles, R. Lindh, F. R. Manby, M Schütz *et al.*, MOLPRO, version 2009.1, a package of *ab initio* programs, 2009, see http://www.molpro.net.
[39] See supplementary material at http://dx.doi.org/10.1063/1.4731883 for vibrational frequencies and moments of inertial of selected points along the minimum energy path for LM1 → ClOO + NO and Pc-ClOO-NO → ClOO + NO computed at the PW91PW91/6-311+G(3df) level of theory.
[40] W. H. Miller, J. Chem. Phys. **65**, 2216 (1976).
[41] D. Chakraborthy, C.-C. Hsu, and M. C. Lin, J. Chem. Phys. **109**, 8887 (1998); Z. F. Xu, C.-H. Hsu, and M. C. Lin, J. Chem. Phys. **122**, 234308 (2005); S. Xu, R. S. Zhu, and M. C. Lin, Int. J. Chem. Kinet. **38**, 322 (2006).
[42] Z. F. Xu, R. S. Zhu, and M. C. Lin, J. Phys. Chem. A. **107**, 1040 (2003).
[43] R. Patrick, and D. M. Golden, Int. J. Chem. Kinet. **15**, 1189 (1983).
[44] J. O. Hirschfelder, C. F. Curtiss, and R. B. Bird, *Molecular Theory of Gases and Liquids*, 2nd ed. (Wiley, New York, 1964).